HHS Public Access

Author manuscript

Nat Med. Author manuscript; available in PMC 2017 September 01.

Published in final edited form as:

Nat Med. 2016 September ; 22(9): 1050–1055. doi:10.1038/nm.4154.

3K3A-APC stimulates post-ischemic neuronal repair by human neural stem cells in mice

Yaoming Wang[1,2,*], **Zhen Zhao**[1,2,*], **Sanket V. Rege**[1,2], **Min Wang**[1,2], **Gabriel Si**[1,2], **Yi Zhou**[3], **Su Wang**[4,5,6], **John H. Griffin**[7,8], **Steven A. Goldman**[4,5,6], and **Berislav V. Zlokovic**[1,2]

[1]Department of Physiology and Biophysics, Keck School of Medicine of the University of Southern California, Los Angeles, CA

[2]Zilkha Neurogenetic Institute, Keck School of Medicine of the University of Southern California, Los Angeles, CA

[3]Department of Neurobiology, Chongqing Key Laboratory of Neurobiology, Third Military Medical University, Shapingba District, Chongqing, China

[4]Center for Translational Neuromedicine, University of Rochester Medical Center, Rochester, New York

[5]Department of Neurology, University of Rochester Medical Center, Rochester, New York

[6]Center for Basic and Translational Neuroscience, University of Copenhagen Faculty of Health and Medical Sciences, Copenhagen 2200, Denmark

[7]Department of Molecular and Experimental Medicine, The Scripps Research Institute, La Jolla, CA

[8]Department of Medicine, Division of Hematology/Oncology, University of California San Diego, San Diego, CA

Abstract

Activated protein C (APC) is a blood protease with anticoagulant activity and cell-signaling activities mediated by activation of protease-activated receptors 1 and 3 (PAR1, PAR3) via non-canonical cleavage[1]. Recombinant APC and/or its analogs with reduced (>90%) anticoagulant activity such as 3K3A-APC (Lys191–193Ala), engineered to reduce APC-associated bleeding risk while retaining normal cell signaling activity, have shown benefits in preclinical models of ischemic stroke[2–6], brain trauma[7], multiple sclerosis[8], amyotrophic lateral sclerosis[9], sepsis[10,11], ischemic/reperfusion injury of heart[12], kidney and liver[13], pulmonary, kidney and gastrointestinal

Address correspondence: Berislav V. Zlokovic, M.D., Ph.D., zlokovic@usc.edu.
*Equally contributed co-first authors

Authors' contributions

Y.W. and Z.Z. designed and performed experiments and analyzed data; Z.Z. contributed to writing the manuscript; S.V.R., M.W. and G.S. performed experiments; Y.Z. customized the Matlab program; J.H.G and S.A.G. edited the manuscript; S.W. and S.A.G. contributed critical materials and comments on the text; B.V.Z. designed all experiments, analyzed data and wrote the manuscript.

Conflict of interest

Dr. Zlokovic is a founder of ZZ Biotech LLC, a biotechnology company with a mission to develop APC and its functional mutants for the treatment of stroke and other neurological disorders. Dr. Griffin is a consultant for ZZ Biotech LLC and inventor for some uses of 3K3A-APC.

inflammation[1,11], diabetes[14] and lethal body radiation[15]. Based on proof of concept studies and an excellent safety profile in humans, 3K3A-APC has advanced to clinical trials as a neuroprotectant in ischemic stroke[16,17]. Recently, 3K3A-APC has been shown to stimulate neuronal production by human neural stem/progenitor cells (NSCs) *in vitro*[18] via a PAR1-PAR3-sphingosine-1-phosphate receptor 1-Akt pathway[19], suggesting the potential for APC-based treatment as a strategy for structural repair in the human central nervous system. Here, we report that late post-ischemic treatment of mice with 3K3A-APC stimulates neuronal production by transplanted human NSCs, promotes circuit restoration, and improves functional recovery. Thus, 3K3A-APC-potentiated neuronal recruitment from engrafted NSCs may offer a new approach to the treatment of stroke and related neurological disorders.

To determine if 3K3A-APC combined with NSC delivery might be developed as an effective combination therapy for neuronal replacement and circuit repair after stroke[20], we studied the effects of late post-ischemic 3K3A-APC treatment on the *in vivo* production of neurons from transplanted NSCs[18,21], and the effects of this combination therapy on long-term neurological recovery and restoration of disrupted neural circuitry in the post-ischemic murine brain. To investigate these processes in mice, we employed the permanent distal middle artery occlusion (dMCAo) model in 8-week old male mice. In contrast to transient occlusion models, this approach produces a highly reproducible, well defined infract lesion in the neocortex[5,6] without the confounding effects of reperfusion. As many stroke patients do not receive thrombolytic tissue-plasminogen activator therapy or arterial thrombectomy for reperfusion after stroke, the Stroke Treatment Academic Industry Roundtable (STAIR) recommends using permanent ischemia models for the development of new therapies for ischemic stroke[22].

Human fetal NSCs transduced with a lentivirus carrying a *CMV-GFP-T2A*-Luciferase cassette (1×10^5 cells) were grafted along the cortical infarct border 7 d after permanent dMCAo in mice[6] (Supplementary Figure 1). Cells were transplanted 7 d after dMCAo because previous work has shown that the acute release of products of tissue damage and death typically subsides within 7 d of dMCAo, providing potentially less hostile graft environment[23]. Additionally, the infarct lesion size is relatively stable 7 d after dMCAo, allowing reproducible transplantation of stem cells in the peri-infarct area[23]. This was followed by intravenous treatment with human recombinant 3K3A-APC (0.2 mg/kg intravenously) or vehicle at 7, 9, 11 and 13 d after stroke, and a daily immunosuppressive treatment with cyclosporine (Fig. 1a). Transplanted NSCs were longitudinally tracked *in vivo* by noninvasive bioluminescence imaging (BLI) of the endogenous luciferase signal (Supplemental Figure 2). BLI showed a progressive decline in luciferase signal in vehicle-treated mice from 100% to 36% within 4 weeks of transplantation, consistent with the reported dying of grafted cells[20] (Fig. 1b, c). In contrast, mice treated with 3K3A-APC showed a time-dependent increase in luciferase signal, with an average of 1.9 and 5.3-fold greater BLI values compared to vehicle at 2 and 5 weeks after stroke, respectively (Fig. 1b, c). These data suggest that 3K3A-APC promotes survival and proliferation of grafted NSCs, consistent with its mitogenic and anti-apoptotic effects[1] previously demonstrated in cultured human NSCs *in vitro*[19]. Similarly, 3K3A-APC supported survival of engrafted NSCs in non-ischemic control mice (Supplemental Figure 3). We also quantified cortical width 5 weeks

after stroke, which is a measure of cerebral cortical expansion or hyperplasia[24–27]. Mice treated with NSCs and 3K3A-APC exhibited a significantly higher cortical width index compared to those treated with NSCs and vehicle, 3K3A-APC alone, or vehicle alone (Fig. 1d, e), These mice also showed significant improvements in motor and sensorimotor functions on rotarod and adhesive removal tests, respectively, at 4 and 5 weeks after stroke (Fig. 1f, g). Altogether, these findings suggest a significant post-ischemic repair potential of late NSCs and 3K3A-APC combination therapy.

We next performed double immunostaining for Tuj1 (a neuronal marker[19]) and $SC121^+$ (a human-specific antigen which detects grafted cells) 5 weeks after stroke and found a 16-fold higher number of $Tuj1^+$ $SC121^+$ co-labeled neuronal-like cells in NSCs and 3K3A-APC-treated mice compared to NSCs and vehicle (Fig. 2a–c). Consistent with previous *in vitro*[19] findings, the differentiation of NSCs into astroglial-like cells was inhibited by 3K3A-APC, evidenced by the lower percentage of $SC121^+$ cells positive for astrocytic glial fibrillary acidic protein[19] in 3K3A-APC-treated mice compared to vehicle (Supplemental Figure 4). Although the survival of transplanted human embryonic kidney 293 cells was also greater in 3K3A-APC-treated mice, this did not lead to neuronal production (Supplementary figure 5a) or improved functional outcomes (Supplementary Figure 5b–c). These findings suggest that functional recovery after NSCs and 3K3A-APC treatment is causally associated with 3K3A-APC-mediated neuronal production from grafted NSCs *in vivo*. To test this notion directly we administered diphtheria toxin (DT)[28] 5 weeks after stroke to ablate all grafted NSCs, which resulted in the complete loss of $SC121^+$ and $Tuj1^+$ $SC121^+$ double positive cells in NSCs and 3K3A-APC-treated mice (Fig. 2d–f). Furthermore, DT-mediated NSC ablation abolished the beneficial effects of 3K3A-APC on post-ischemic neurological recovery (Fig. 2g–h) and cortical expansion (Fig. 2i). These data suggest that transplanted NSCs directly contributed to functional recovery[20,28] after 3K3A-APC treatment.

Next, we utilized anterograde labeling with adeno-associated viruses (AAV2/9.TurboRFP) to trace axonal projections from the primary motor cortex M1 (a major source of intracortical input to primary somatosensory cortex S1) to the S1 region that is typically damaged by dMCAo (Supplemental Figure 6; see Methods). In contrast to the scarcity of axonal projections found in mice treated with NSCs and vehicle, we observed substantial $TurboRFP^+$ M1 axonal projections to stroke-damaged S1 in NSCs and 3K3A-APC-treated mice. These M1 axons were intermingled with engrafted human $SC121^+$ cells (Fig. 3a) and were closely juxtaposed to NSCs-derived $Tuj1^+$ neuronal-like cells (Fig. 3b–c). Quantitative analysis revealed a 9-fold higher amount of these putative contacts.in NSCs and 3K3A-APC-treated mice compared to vehicle (Fig. 3d). Staining for synaptic markers demonstrated a higher number of co-localized pre-synaptic (synaptophysin) and post-synaptic (PSD-95) puncta on the engrafted $SC121^+$ NSCs in 3K3A-APC-treated mice compared to vehicle (Fig. 3e–f), suggesting the formation of synapses between host neurons and NSC-derived neurons. To examine the degree of functional circuitry present in stroke-affected S1, we performed *in vivo* voltage-sensitive dye (VSD) imaging of cortical membrane potentials 5 weeks after dMCAo in the forelimb S1 region evoked by mechanical stimulation of the contralateral forelimb (Fig. 3g). We observed stronger evoked transient depolarizations in NSCs and 3K3A-APC-treated mice (Fig. 3h), evidenced by a larger peak VSD response amplitude and shorter time to peak response compared to either NSCs and

vehicle-treated mice or dMCAo-alone mice (Fig. 3i–j, Supplemental Figure 7). NSCs and 3K3A-APC treatment yielded a complete rescue of time to peak response, while peak response amplitudes were rescued to 56% of that observed in sham-operated controls.

To better assess the functional integration of NSCs into the host neuronal circuitry, we stably transduced NSCs with a lentivirus carrying the intracellular calcium indicator GCaMP3 (CAG-GCaMP3-Puro-WPRE[29]; Supplementary Figure 8a–b, see Methods), and transplanted GCaMP3-expressing NSCs (1×10^5 cells) along the cortical infarct border 7 d after dMCAo. This was followed by 3K3A-APC (0.2 mg/kg) or vehicle treatment at 7, 9, 11 and 13 d after stroke. We then imaged the evoked GCaMP3 signal through a cranial window preparation overlying the affected S1 region in response to contralateral forelimb mechanical stimulation 5 weeks after stroke (Supplementary Figure 8c). We found that transplanted GCaMP3-NSCs in the primary sensory S1 cortex responded to forelimb stimulation with an increase in transcranial GFP fluorescence within 1 s (Figure 4a–b), exhibiting a profile comparable to that previously reported for the mesoscale transcranial neuronal activity mapping with GCaMP3[30]. Mice treated with NSCs and 3K3A-APC showed 3-fold greater average peak amplitude compared to vehicle (Figure 4a–c). In addition, deep multi-photon laser-scanning microscopy indicated that individual GCaMP3-NSCs in the S1 cortical layers II-III responded to forelimb sensory stimulation (Supplementary Figure 8d), and their response profiles (Supplementary Figure 8e) resembled the typical profiles of GCaMP3-based responses from mature mouse cortical neurons[31]; these differ from astrocytic responses that usually last > 10 s[32]. NSCs and 3K3A-APC-treated mice exhibited a 6-fold greater percentage of GCaMP3-positive NSCs that responded to sensory stimulation compared to vehicle (Figure 4d), which correlated with a greater than 5-fold increase in the percentage of GCaMP3-positive cells expressing the neuronal markers MAP2 or Tuj1 in 3K3A-APC-treated mice compared to vehicle (Figure 4e–f). These data provide a strong support for the improved functional integration of grafted NSCs into the host neuronal circuitry as a result of 3K3A-APC-treatment.

FACS analysis of mouse brains after the GCaMP3 imaging experiments, using the GFP signal for gating of GCaMP3-positive cells (Supplementary Fig. 9a) and human CD31 as a marker for NSC-derived endothelial cells, indicated that < 1% of GCaMP3-NSCs expressed human endothelial CD31 five weeks after stroke (Supplementary Figure 9b), which was also corroborated by negative human-specific CD31 endothelial immunoreactivity (Supplementary Figure 9c). As suggested by previous reports demonstrating the angiogenic activity of APC[4] and the secretion of angiogenic growth factors by NSCs[33], both 3K3A-APC and NSCs separately promoted murine-derived neovascularization, as shown by 30–40% and 25–30% increases in murine CD31-positive microvascular profiles and lectin-positive perfused microvascular length after *in vivo* lectin angiography[4], respectively (Supplementary Figure 9d–f). However, NSC and 3K3A-APC combination treatments did not have an additive effect on murine neovascularization or cerebral perfusion (Supplementary Figure 9d–f). In contrast, combined 3K3A-APC and NSC treatment led to significant functional improvements compared to 3K3A-APC alone or NSC treatment alone that had no significant effects (Fig. 1f–g). Moreover, ablation of NSCs with diphtheria toxin (Fig. 2d–h) suggests that functional improvements of 3K3A-APC and NSCs combination therapy depends exclusively on the existence of transplanted NSCs, but not on indirect

contribution from the host endogenous cells (not affected by DT). Together, these data suggest that grafted human NSCs do not produce human endothelial cells[34] in 3K3A-APC-treated mice, and that the improved murine neovascularization is not sufficient to lead to functional improvements, but rather that functional benefit requires 3K3A-APC-potentiated neuronal production from transplanted NSCs, and a functional integration of those new neurons into the host neural circuits.

Regenerative therapies with human NSCs hold great promise for human CNS diseases[35], but the issue of immunogenicity of allogeneic transplants remains[36]. Using immunosuppressive treatment with cyclosporine, we have observed both good transplantation tolerance and functional benefit (Fig. 1a–c), suggesting that this approach may be appropriate for clinical translation in stroke. As 3K3A-APC has been shown to be neuroprotective in models of larger strokes in rodents with stroke risk factors, and in females and aged rodents[6], one would expect that 3K3A-APC and NSCs repair therapy would successfully translate to different experimental stroke models and humans[22].

In summary, our data show that APC agonist-based clinical therapeutics such as 3K3A-APC may strongly potentiate the *in vivo* integration and neurogenic activity of transplanted human NSCs. This observation may be of interest not only in the repair of stroke-damaged neural circuits, but also in regards to NSC delivery for the broader range of neurological disorders involving discrete neuronal loss.

Online Methods

Animals

Eight-week-old male C57BL/6J mice were used in this study. Mice were housed in plastic cages on a 12 h light cycle with ad libitum access to water and a standard laboratory diet. The Institutional Animal Care and Use Committee at the University of Southern California according to the National Institutes of Health guidelines approved all procedures. All the animals that survived surgical procedures were included in the study. All animals were randomized for all stroke studies and treatments. All experiments were blinded; the operators responsible for experimental procedure and data analysis were blinded and unaware of group allocation throughout the experiments.

Distal Middle Cerebral Artery Occlusion (dMCAo)

Mice were anesthetized with 100 mg/kg Ketamine intraperitoneally (IP) and 5–10 mg/kg IP xylazine, using a 27-½ gauge needle. Rectal temperature was maintained at 37°C using a feedback-controlled heating system. A 1 mm incision was made to expose the skull. A modified permanent dMCAo technique was used as previously described[6]. Briefly, under the surgical microscope, the left common carotid artery was isolated through a neck incision and ligated using a 5–0 silk. The left distal middle cerebral artery was exposed through a craniotomy and permanently cauterized above the rhinal fissure. This model of ischemia produces a focal infarct in mice generally localized to the neocortex and the distribution of the ischemic lesion at the level of optic chiasm reproducibly involves the primary

somatosensory cortex region S1 including the forelimb (S1FL) region and the secondary somatosensory S2 region in both mice[6] and rats[37].

Human NSCs culture

Human fetal brain was taken from aborted fetuses of 15–22 weeks gestational age, under a protocol approved by the Research Subjects Review Board of the University of Rochester Medical Center, as previously described[18,19]. The samples were collected into Ca/Mg-free Hank's buffered saline solution (HBSS) and dissected to separate the telencephalic VZ/SVZ from non-ventricular parenchyma, and dissociated[18]. The cells were resuspended in DMEM/F12/N2 supplemented with 20 ng/ml (1.4 nM) bFGF (Sigma, St. Louis, MO), plated in low attachment T-25 flask (Corning, Acton, MA) and maintained as neurospheres. The multilineage competence and sustained *in vitro* self-renewal of these cells, their neural stem cell phenotype and their neurogenic potential *in vivo* have all been previously described[18,21]. On the day of injection, the neural stem cells (NSCs) (passage 2) were dissociated with StemPro Accutase (Invitrogen, Catalog #A11105-01) into single-cell suspension in DMEM/F12/N2 medium lacking growth factor.

Human NSCs Transplantation

All mice including controls received immunosuppressant cyclosporine (Norvartis, Sandimmune 10 mg/kg, i.p.) daily. Seven days after dMCAo, mice were anesthetized placed in a stereotactic apparatus (ASI Instruments, Inc., USA) and were fixed accordingly. The skull was exposed and a hole was drilled at the appropriate position on the ischemic hemisphere. 1×10^5 NSCs in a total volume of 1 μl were microinjected along the anterior-posterior axis (three points at the infarct border) into the cortex at a rate of 0.1 μl/min, using an infusion pump (World Precision instruments). The injection coordinates were: point #1, 1 mm anterior to bregma and 2 mm ventral to the brain surface; point #2, 0 mm anterior to bregma and 2 mm ventral to the brain surface; point #3, 1 mm posterior to bregma and 1.8 mm ventral to the brain surface. Human 3K3A-APC (0.2 mg/kg, i.v.) or vehicle was administered at 7, 9, 11, and 13 d post-stroke, as previously described[5,6].

In vivo imaging of transplanted cells

Bioluminescent and fluorescent lentivirus (*pGreenFire: CMV-GFP-T2A-Luciferase*) were purchased from System Biosciences, Catalog # BLIV101VA-1. For transduction, 0.5×10^6 single cells in 300 μl of DMEM-F12 medium were inoculated with one viral stock ($>2\times10^9$ IFUs) for 1 hour at 37 °C, 5% CO_2 in a humidified atmosphere with agitation every 10–15 minutes, before transferred to T25 flask (Corning). After 24 h, the viral containing medium was replaced with complete medium. Transduced neurospheres were collected after 3–4 d and dissociated with StemPro Accutase for transplantation. Efficiency of transduction was also determined by flow cytometry. 70–80% GFP-positive cells were observed in all cultures. Bioluminescent *in vivo* imaging experiments were performed at using a cooled CCD optical macroscopic imaging system (Xenogen-IVIS), as described previously[28].

Assessment of cerebral cortical expansion

Mice anesthetized as above were perfusion fixed with paraformaldehyde 5 weeks after stroke and the brains were removed. Whole brain images were captured using a microscopic digital camera system coupled to a dissecting stereomicroscope (AxioCam, Zeiss). Images were analyzed by the NIH Image J system (Bethesda, MD, USA). The distance from midline to the edge of brain on the infarcted hemisphere (x) was divided by the distance from midline to the lateral edge on the contralateral, non-infarcted hemisphere (y) to calculate the cortical width index (x / y) as previously described[24–27].

Behavioral Tests

Rotarod Test—Mice were trained on an accelerating (5–15 rpm) rotating rod (rotarod) for 3 d before dMCAo; only those mice able to remain on the rod for 200 s at 15 rpm underwent dMCAo. Test sessions consisting of four trials at 15 rpm were carried out immediately before dMCAo and 1, 7, 14, 21, 28, and 35 d later by an investigator who was blinded to the experimental groups. The final score was expressed as the mean time that a mouse was able to remain on the rod over four trials, as we previously described[38].

Adhesive removal test—The adhesive removal test measures sensorimotor function. A small piece of adhesive tape (3 mm × 4 mm) was placed on the forepaw contralateral to the stroke hemisphere. Time taken to contact and remove adhesive tape was recorded, with a maximum of 120 s. Three trials were performed at 0, 1, 7, 14, 21, 28, and 35 d after stroke, and the mean time of three trials was used to do analysis[6,39,40].

Ablation of transplanted NSCs—Cell ablation experiments were performed as described previously[28,41,42]. Diphtheria toxin (DT) was purchased from Sigma (Catalog#D0564). Five weeks after dMCAo, DT solution (50 μg/kg) or vehicle was administered to mice by intraperitoneal injection, daily for two days. Mice were reassessed for behavioral tests within one week of DT or vehicle administration and sacrificed for histological analysis. The DT dosing regimen as used in the present study did not lead to any functional deficits or structural changes after dMCAo in control mice treated only with DT consistent with previous reports in control mice in other models of neurological disorders treated with DT[28].

HEK 293 cell culture and transplantation—HEK293 cells (ATCC, CRL-1573) were cultured in Eagle's Minimum Essential Medium supplemented with 10% fetal bovine serum, following supplier's protocol and tested free of mycoplasma contamination. 1×10^5 cells in a total volume of 1 μl were microinjected following the same protocol listed above for NSCs.

Tissue staining—Animals were transcardially perfused with PBS followed by 4% PFA. Brains were postfixed overnight in the same fixative at 4 °C. For cryosectioning, fixed tissues were cryoprotected in 30% sucrose in PBS overnight at 4 °C, and embedded in OCT compound (Tissue Tek). Cryostat sections were cut at 20 μm thickness from the center of the lesion (bregma −1 to +1 mm). Three cross sections per mouse, at the levels of bregma −1, 0 and +1 mm, were selected and permeabilized in PBS-T (PBS containing 0.2% Triton X-100) for 10 min, blocked with 5% normal goat serum (Jackson ImmunoResearch, Catalog

#017-000-121) for 60 min and incubated in primary antibody diluted in blocking solution overnight at 4°C. Primary antibodies used in this study include: rabbit monoclonal anti-Tuj1 (1:100, Cell Signaling Catalog #5568), rat monoclonal anti-glial fibrillary acidic protein (GFAP) (1:200, Invitrogen Catalog #13-0300). Mouse monoclonal antibody specific for human cytoplasmic marker (Clone SC121, 1:500, StemCells, Inc. Catalog #AB-121-U-050) were used together with Mouse on Mouse (M.O.M) kit (Vector Laboratories, Catalog #BMK-2202) to stain for transplanted human NSCs. After three washes with PBS, they were incubated with the secondary antibodies for 1 h, which are Alexa 488-conjugated donkey anti-mouse (1:200, Invitrogen, Catalog#A21202), Alexa 568-conjugated donkey anti-rabbit (1:200, Invitrogen, Catalog#A10042). After being rinsed with PBS, nuclei were stained with DAPI. Validation is provided on the manufacturer's website. All images were taken with a Zeiss 510 confocal microscopy or using the BZ 9000 all-in-one Fluorescence Microscope from Keyence (Osaka, Japan), and analyzed using NIH Image J software. The region of interest for cell counting was the ischemia-affected S1 region. Data from randomly selected 3 sections (100 μm apart) were averaged for each mouse, and 5 mice per group were statistically compared. For cell counting in Fig. 2c, e, and f, we analyzed the total number of cells per section.

Viral injection for anterograde labeling—Animals were anesthetized with 1.0–1.5% isofluorane for the duration of the surgery. Animals were fixed to a stereotaxic frame and a ~3 cm rostral-caudal incision cut to expose the scalp. The skull was cleaned and dried with 70% alcohol, then a small cranial window was opened at coordinates 3.2,-1.5,-0.45 mm (x,y,z) with a drill, diameter 3 mm. recombinant Adeno-associated virus serotype 2/9 (Penn Vector Core, Catalog # AV-9-PV2642) was withdrawn into a pulled glass pipette, diameter 0.5 mm, filled with mineral oil. The needle was inserted into the cranial window at the rate of 1mm/min, 2 min were allowed for the parenchyma to seal over the needle, and then 50 nL of the virus was pressure injected at the rate of 10 nL/min via digital controller (World Precision Instruments, Catalog # UMP3-1). Two min were allowed for viral diffusion, and the needle was then withdrawn at the rate of 1 mm/min. The window was sealed with bone wax (Lukens #SUS901), the scalp sutured closed, then animal was placed under heat lamp to recover from anesthesia. Animals were housed for recovery and virus propagation for 21 d, before sacrificing for histological analysis. In brief, brains were postfixed overnight in PFA at 4 °C, and vibratome sectioned at 25 μm thickness. Sections, with TurboRFP labeling in the lesioned area (bregma −1 to +1 mm) were collected and stained with SC121 and Tuj1 antibodies before confocal analysis.

A tiled Z-stack image at 1 μm intervals was acquired for each section, covering the area that included both $SC121^+$ cells and $TurboRFP^+$ axons. The region of interest was ischemia-affected S1 cortex. A contact between grafted neuron-like cells and axonal projection was defined as adjacent signal between $SC121^+$ $Tuj1^+$ cells and $TurboRFP^+$ labeled axons from orthogonal view in 4 consecutive optical sections (>1 μm) per mouse and from 5 animals per group. An example of contact is shown in Figure 3c. The number of contacts were manually counted for each section and statistically compared between groups by Student's t-test.

Quantifying Synapses—Using compartment-specific antibodies for synaptophysin (presynaptic marker, 1:100, Sigma Catalog #SAB4502906) and PSD-95 (postsynaptic marker, 1:100, Santa Cruz Biotechnology Catalog sc-6926) we labeled both presynaptic terminals as well as sites of postsynaptic specialization in grafted NSCs. Synapses were defined as co-localized puncta for both presynaptic and postsynaptic markers on NSCs, as previously reported[43]. The region of interest is the infarcted cortex. Images were obtained on a Zeiss LSM 510 using a 63x oil immersion objective. $SC121^+$ 2 cells per image, 5 images per section, 1 section per mouse at the level of the optic chiasm and 5 animals per group were selected for synapse counting. The number of synapses was quantified using ImageJ.

Voltage-sensitive dye imaging (VSD)—Animals were anesthetized with 3.0% isofluorane vaporized in air using the SomnoSuite Small Animal Anesthesia System (Kent Scientific Catalog # SOMNO). Anesthesia was then maintained at 1.0–1.5% isofluorane for the duration of the surgery, with head fixed in a stereotaxic frame (Kopf Instruments). A circular cranial window was drilled over the S1 region of the somatosensory cortex (center at AP = −0.94 mm, L = 1.5 mm), then RH-1692 VSD (Optical Imaging) dissolved in artificial cerebrospinal fluid (aCSF) was applied to the exposed cortex for 90 min. The brain was then washed with aCSF and cover-slipped with a 3 mm circular glass coverslip sealed using low-melt agarose (~2%) dissolved in aCSF. Images were captured at 10 ms/frame using a 1/2 inch MiCAM02-HR CMOS camera (SciMedia) coupled with MiCAM acquisition software (SciMedia). RH-1692 was excited using a MHAB-150W (Moritex Corp.) light source with a 632/22 nm filter, and fluorescence collected with a 665 nm long-pass filter. The contralateral forelimb was stimulated by a mechanical vibration lasting 300 ms. Alternating image sets were taken with and without stimulus to generate “stimulus trial” and “baseline” responses. Next the baseline image set was subtracted from the stimulus trials to eliminate background signal and shift-over-time in each trial. 10 baseline subtracted trials were averaged to make up the final profile for each experiment. Each frame of a trial and the average intensity of each frame were plotted using a custom-made Matlab program (Mathworks Inc.). The change in fluorescent VSD signal was calculated as a percentage change by dividing the signal intensity after stimulation by the average intensity before stimulation (ΔF / F0). The peak amplitude of fluorescent change in a trial and the interval between stimulation onset and response peak were also measured using the same program.

In vivo GCaMP3 imaging

GCaMP3 is a green fluorescent protein (GFP)-based calcium sensor that has been frequently used for imaging calcium dynamics in living cells including imaging of neural activity in worms, flies and mice[27]. Lenti-CAG-GCaMP3-Puro-WPRE viruses were purchased from Cellomics Technology (Catalog # PLV-10076-50, titter: 1×10^8 CFU/ml). Puromycin (1 μg/mL) selection started 3 d after transduction and continued for 7 d. Neurospheres were then collected and dissociated for transplantation. Efficiency of transduction was determined by flow cytometry using a regular setting for GFP. Approximately 90% GCaMP3-positive cells were observed in all transduced NSCs cultures.

We injected GCaMP3-NSCs (1×10^5 cells) along the cortical infarct border 7 d after permanent dMCAo followed by intravenous treatment with human recombinant 3K3A-APC

(0.2 mg/kg intravenously) or vehicle 7, 9, 11 and 13 d after stroke. Next, we imaged the evoked GCaMP3 signal in response to forelimb mechanical stimulation of S1 region 5 weeks after stroke using both a transcranial setting with the MiCAM02-HR CMOS camera and deep cortical setting with two-photon laser scanning microscope. In these experiments mice were anesthetized with isoflurane, placed in a stereotaxic frame, and imaged through a cranial window over the S1 region as described above.

Transcranial activity mapping of GCaMP3 signal was performed as previously described[30]. Images of the cortical surface were recorded at 33 ms/frame using a 1/2 inch MiCAM02-HR CMOS camera (SciMedia) coupled with MiCAM acquisition software (SciMedia). Calcium indicators were excited with blue-light-emitting diodes (Luxeon, 470 nm) with bandpass filters (467–499 nm). Emission fluorescence was filtered using a 510–550 nm bandpass filter. The contralateral forelimb was stimulated by a mechanical vibration lasting 300 ms. To calculate the calcium response evoked by stimulation, 10 trials separated by a 10 s interval were collected, averaged and normalized to the average baseline recorded before stimulation, using a custom-made Matlab program. The change in fluorescent GFP signal was calculated as a percentage change by dividing the signal intensity after stimulation by the average intensity before stimulation (ΔF / F0). The peak amplitude of fluorescent change in a trial and the interval between stimulation onset and response peak were also measured using the same program.

In vivo deep cortical imaging of GCaMP3-positive grafted cells was performed on a two-photon laser-scanning microscope (LSM 5 MP) with a Mai-Tai 80 femtosecond pulsed laser (Spectra-Physics) running at 900 nm for GCaMP3, as previously described[31]. Images (128 × 128 pixels) were collected at 4 Hz. To calculate the calcium response evoked by stimulation, 10 trials separated by a 10 s interval were collected, averaged and normalized to the average baseline recorded before stimulation, using a custom-made Matlab program. The change in fluorescent GFP signal was calculated as a percentage change by dividing the signal intensity after stimulation by the average intensity before stimulation (ΔF / F0). The peak amplitude of fluorescent change in a trial and the interval between stimulation onset and response peak were also measured using the same program. The region of interest was the S1 region. In each mouse individual GCaMP3-NSCs cell responses to forelimb stimulus were determined from 20–30 cells. 5 mice were compared between groups.

Flow cytometry

Quantitative flow cytometry analyses were performed using the Attune NxT Acoustic Focusing Cytometer, as we previously described[19]. Briefly, the cells were harvested from in vitro cultures or collected after dissection of ischemic brain regions with transplants, and stained with various markers as indicated, following a standard indirect flow cytometry protocol (Abcam). Quantitative analyses were performed using the Attune® Cytometric Software. PE-conjugated mouse anti-human CD31 (1:50; BD Pharmingen, clone WM59, #555446; minimal cross reactivity with murine endogenous CD31) was used.

In vivo lectin-FITC angiography

Dylight 488-labeled L. esculentum (tomato) lectin at 10 mg/kg was administered via the femoral vein in anesthetized mice 5 min before killing[4], five weeks after dMCAo. For the analysis of blood vessels, sections from brains that were used for *in vivo* lectin-FITC angiography were incubated with an antibody specific to murine CD31 (1:50; Invitrogen, #RM5200) overnight at 4°C followed by incubation with the secondary antibodies (TRITC-conjugated donkey anti-rat IgG; 1:200; Invitrogen #A18750). Total microvascular length was calculated using the NeuronJ plugin for ImageJ, as previously described[4].

Statistics

Sample sizes were calculated using nQUERY assuming a two-sided alpha-level of 0.05, 80% power, and homogeneous variances for the 2 samples to be compared, with the means and common standard deviation for different parameters predicted from published data and our previous studies. Data are presented as mean ± s.d., or means ± s.e.m. as indicated in the figure legends. For comparison between two groups, F test was conducted to determine the similarity in the variances between the groups that are statistically compared, and statistical significance was analyzed by Student's t-test. For multiple comparisons, Bartlett's test for equal variances was used to determine the variances between the multiple groups and one-way analysis of variance (ANOVA) followed by Bonferroni's post hoc test was used to test statistical significance, using GraphPad Prism software. A *P* value of less than 0.05 was considered statistically significant.

Supplementary Material

Refer to Web version on PubMed Central for supplementary material.

Acknowledgments

The authors want to acknowledge the NIH grants 9R01NS090904-16 (B.V.Z.), RO1HL052246 and PO1 HL031950 (J.H.G.), R01NS75345 (S.A.G.); National Natural Science Foundation of China grant 31371116 (Y.Z.); and grants from the Adelson Medical Research Foundation, New York State Stem Cell Research Board (NYSTEM), Novo Nordisk Foundation, Lundbeck Foundation, National Multiple Sclerosis Society, and ALS Association (S.A.G.).

References

1. Griffin JH, Zlokovic BV, Mosnier LO. Activated protein C: biased for translation. Blood. 2015; 125:2898–2907. [PubMed: 25824691]
2. Cheng T, et al. Activated protein C blocks p53-mediated apoptosis in ischemic human brain endothelium and is neuroprotective. Nat Med. 2003; 9:338–342. [PubMed: 12563316]
3. Cheng T, et al. Activated protein C inhibits tissue plasminogen activator-induced brain hemorrhage. Nat Med. 2006; 12:1278–1285. [PubMed: 17072311]
4. Thiyagarajan M, Fernández JA, Lane SM, Griffin JH, Zlokovic BV. Activated protein C promotes neovascularization and neurogenesis in postischemic brain via protease-activated receptor 1. J Neurosci Off J Soc Neurosci. 2008; 28:12788–12797.
5. Wang Y, et al. An activated protein C analog with reduced anticoagulant activity extends the therapeutic window of tissue plasminogen activator for ischemic stroke in rodents. Stroke J Cereb Circ. 2012; 43:2444–2449.

6. Wang Y, et al. Activated protein C analog protects from ischemic stroke and extends the therapeutic window of tissue-type plasminogen activator in aged female mice and hypertensive rats. Stroke J Cereb Circ. 2013; 44:3529–3536.
7. Walker CT, et al. Activated protein C analog with reduced anticoagulant activity improves functional recovery and reduces bleeding risk following controlled cortical impact. Brain Res. 2010; 1347:125–131. [PubMed: 20513369]
8. Han MH, et al. Proteomic analysis of active multiple sclerosis lesions reveals therapeutic targets. Nature. 2008; 451:1076–1081. [PubMed: 18278032]
9. Winkler EA, et al. Blood-spinal cord barrier disruption contributes to early motor-neuron degeneration in ALS-model mice. Proc Natl Acad Sci U S A. 2014; 111:E1035–1042. [PubMed: 24591593]
10. Taylor FB, et al. Protein C prevents the coagulopathic and lethal effects of Escherichia coli infusion in the baboon. J Clin Invest. 1987; 79:918–925. [PubMed: 3102560]
11. Esmon CT. Protein C anticoagulant system—anti-inflammatory effects. Semin Immunopathol. 2012; 34(1):127–132. [PubMed: 21822632]
12. Loubele STBG, et al. Activated protein C protects against myocardial ischemia/ reperfusion injury via inhibition of apoptosis and inflammation. Arterioscler Thromb Vasc Biol. 2009; 29:1087–1092. [PubMed: 19372456]
13. Park SW, Chen SWC, Kim M, D'Agati VD, Lee HT. Human activated protein C attenuates both hepatic and renal injury caused by hepatic ischemia and reperfusion injury in mice. Kidney Int. 2009; 76:739–750. [PubMed: 19625989]
14. Isermann B, et al. Activated protein C protects against diabetic nephropathy by inhibiting endothelial and podocyte apoptosis. Nat Med. 2007; 13:1349–1358. [PubMed: 17982464]
15. Geiger H, et al. Pharmacological targeting of the thrombomodulin-activated protein C pathway mitigates radiation toxicity. Nat Med. 2012; 18:1123–1129. [PubMed: 22729286]
16. Lyden P, et al. Phase 1 Safety, Tolerability and Pharmacokinetics of 3K3A-APC in Healthy Adult Volunteers. Curr Pharm Des. 2013; 19:7479–7485. [PubMed: 24372304]
17. ClinicalTrials.gov. Bethesda (MD): National Library of Medicine (US); 2014 Aug 18. [Internet]Identifier NCT02222714, Safety evaluation of 3K3A-APC in ischemic stroke (RHAPSODY);https://clinicaltrials.gov/ct2/show/NCT02222714
18. Wang S, et al. Prospective identification, isolation, and profiling of a telomerase-expressing subpopulation of human neural stem cells, using sox2 enhancer-directed fluorescence-activated cell sorting. J Neurosci Off J Soc Neurosci. 2010; 30:14635–14648.
19. Guo H, et al. An Activated Protein C Analog Stimulates Neuronal Production by Human Neural Progenitor Cells via a PAR1-PAR3-S1PR1-Akt Pathway. J Neurosci. 2013; 33:6181–6190. [PubMed: 23554499]
20. Savitz SI. Cell therapies: careful translation from animals to patients. Stroke J Cereb Circ. 2013; 44:S107–109.
21. Keyoung HM, et al. High-yield selection and extraction of two promoter-defined phenotypes of neural stem cells from the fetal human brain. Nat Biotechnol. 2001; 19:843–850. [PubMed: 11533643]
22. Albers GW, et al. Stroke Treatment Academic Industry Roundtable (STAIR) Recommendations for Maximizing the Use of Intravenous Thrombolytics and Expanding Treatment Options With Intra-arterial and Neuroprotective Therapies. Stroke. 2011; 42:2645–2650. [PubMed: 21852620]
23. Kelly S, et al. Transplanted human fetal neural stem cells survive, migrate, and differentiate in ischemic rat cerebral cortex. Proc Natl Acad Sci. 2004; 101:11839–11844. [PubMed: 15280535]
24. Taguchi A, et al. Administration of CD34+ cells after stroke enhances neurogenesis via angiogenesis in a mouse model. J Clin Invest. 2004; 114:330–338. [PubMed: 15286799]
25. Zhao BQ, et al. Role of matrix metalloproteinases in delayed cortical responses after stroke. Nat Med. 2006; 12:441–445. [PubMed: 16565723]
26. Wen Z, Wang P. Recombinant human erythropoietin increases cerebral cortical width index and neurogenesis following ischemic stroke. Neural Regen Res. 2012; 7:578–582. [PubMed: 25745447]

27. Wang Y, et al. Activated protein C analog promotes neurogenesis and improves neurological outcome after focal ischemic stroke in mice via protease activated receptor 1. Brain Res. 2013; 1507:97–104. [PubMed: 23438513]
28. Abematsu M, et al. Neurons derived from transplanted neural stem cells restore disrupted neuronal circuitry in a mouse model of spinal cord injury. J Clin Invest. 2010; 120:3255–3266. [PubMed: 20714104]
29. Tian L, et al. Imaging neural activity in worms, flies and mice with improved GCaMP calcium indicators. Nat Methods. 2009; 6:875–881. [PubMed: 19898485]
30. Vanni MP, Murphy TH. Mesoscale transcranial spontaneous activity mapping in GCaMP3 transgenic mice reveals extensive reciprocal connections between areas of somatomotor cortex. J Neurosci Off J Soc Neurosci. 2014; 34:15931–15946.
31. Zariwala HA, et al. A Cre-dependent GCaMP3 reporter mouse for neuronal imaging in vivo. J Neurosci Off J Soc Neurosci. 2012; 32:3131–3141.
32. Li D, Agulhon C, Schmidt E, Oheim M, Ropert N. New tools for investigating astrocyte-to-neuron communication. Front Cell Neurosci. 2013; 7:193. [PubMed: 24194698]
33. Horie N, et al. Transplanted stem cell-secreted vascular endothelial growth factor effects poststroke recovery, inflammation, and vascular repair. Stem Cells Dayt Ohio. 2011; 29:274–285.
34. Wurmser AE, et al. Cell fusion-independent differentiation of neural stem cells to the endothelial lineage. Nature. 2004; 430:350–356. [PubMed: 15254537]
35. Goldman SA. Stem cell therapeutics for neurological disease: Facts, fantasies, and wishful thinking. Cell Stem Cell. 2016; 18:174–188. [PubMed: 26849304]
36. Fuchs EJ. Transplantation tolerance: from theory to clinic. Immunol Rev. 2014; 258:64–79. [PubMed: 24517426]
37. Markgraf CG, et al. Recovery of sensorimotor function after distal middle cerebral artery photothrombotic occlusion in rats. Stroke J Cereb Circ. 1994; 25:153–159.
38. Winkler EA, et al. Blood-spinal cord barrier disruption contributes to early motor-neuron degeneration in ALS-model mice. Proc Natl Acad Sci U S A. 2014; 111:E1035–1042. [PubMed: 24591593]
39. Bouet V, et al. The adhesive removal test: a sensitive method to assess sensorimotor deficits in mice. Nat Protoc. 2009; 4:1560–1564. [PubMed: 19798088]
40. Freret T, et al. Behavioral deficits after distal focal cerebral ischemia in mice: Usefulness of adhesive removal test. Behav Neurosci. 2009; 123:224–230. [PubMed: 19170448]
41. Furukawa N, Saito M, Hakoshima T, Kohno K. A diphtheria toxin receptor deficient in epidermal growth factor-like biological activity. J Biochem (Tokyo). 2006; 140:831–841. [PubMed: 17071947]
42. Saito M, et al. Diphtheria toxin receptor-mediated conditional and targeted cell ablation in transgenic mice. Nat Biotechnol. 2001; 19:746–750. [PubMed: 11479567]
43. Ullian EM, et al. Control of Synapse Number by Glia. Science. 2001 Jan 26; 291(5504):657–661. [PubMed: 11158678]

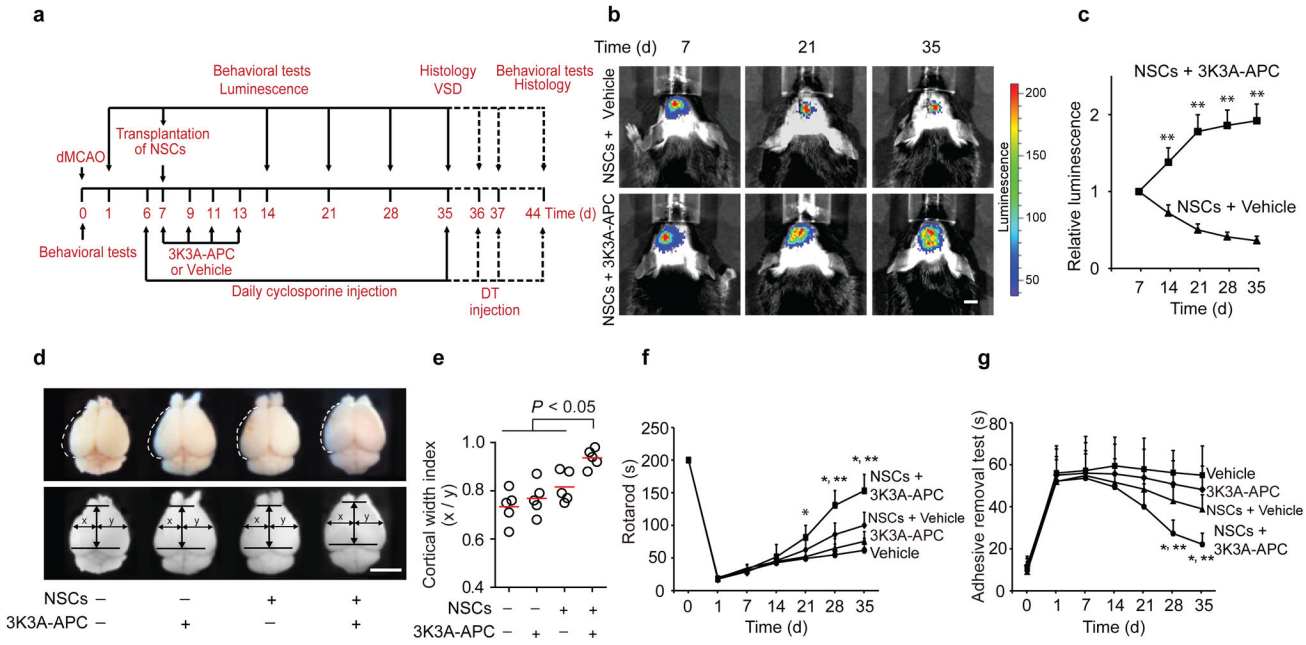

Figure 1. Promotion of NSC transplant survival by late 3K3A-APC treatment improves structural and functional outcomes after distal middle cerebral artery occlusion (dMCAo)

(**a**) Experimental design: NSCs were transplanted 7 d after stroke. Intravenous 3K3A-APC (0.2 mg/kg) or vehicle was administered 7, 9, 11 and 13 d after stroke. All mice received intraperitoneal cyclosporine (10 mg/kg daily). Outcome parameters were measured at the indicated times. VSD, voltage-sensitive dye imaging. (**b–c**) Bioluminescence imaging (**b**) and *in vivo* quantification of luciferase signal (**c**) from engrafted NSCs transduced with a CMV-GFP-T2A-Luciferase lentivirus. Scale bar = 5 mm; mean ± s.d.; $n = 5$ mice per group; $^{**}P < 0.05$, NSCs + 3K3A-APC versus NSCs + vehicle by Student's t-test. (**d–e**) *Ex vivo* images (**d**) and scatter plot (**e**) of cortical width index 35 d after dMCAo and NSCs and 3K3A-APC treatment compared to vehicle-alone, 3K3A-APC alone, and NSCs plus vehicle; x and y mark the maximum width from the midline to the edge of the infarcted and non-infarcted hemispheres, respectively. Scale bar = 5 mm. n = 5 mice per group; $P < 0.05$ by one-way ANOVA followed by Bonferroni's post hoc test. (**f–g**) The rotarod test (**f**) and adhesive removal test (**g**) after vehicle-alone, 3K3A-APC alone, NSCs and vehicle or NSCs and 3K3A-APC. In **f** and **g**, mean ± s.d.; $n = 5$ mice per group; $^{*}P < 0.05$, NSCs + 3K3A-APC versus vehicle or 3K3A-APC alone; $^{**}P < 0.05$, NSCs + 3K3A-APC versus NSCs + vehicle by one-way ANOVA and Bonferroni's post hoc test.

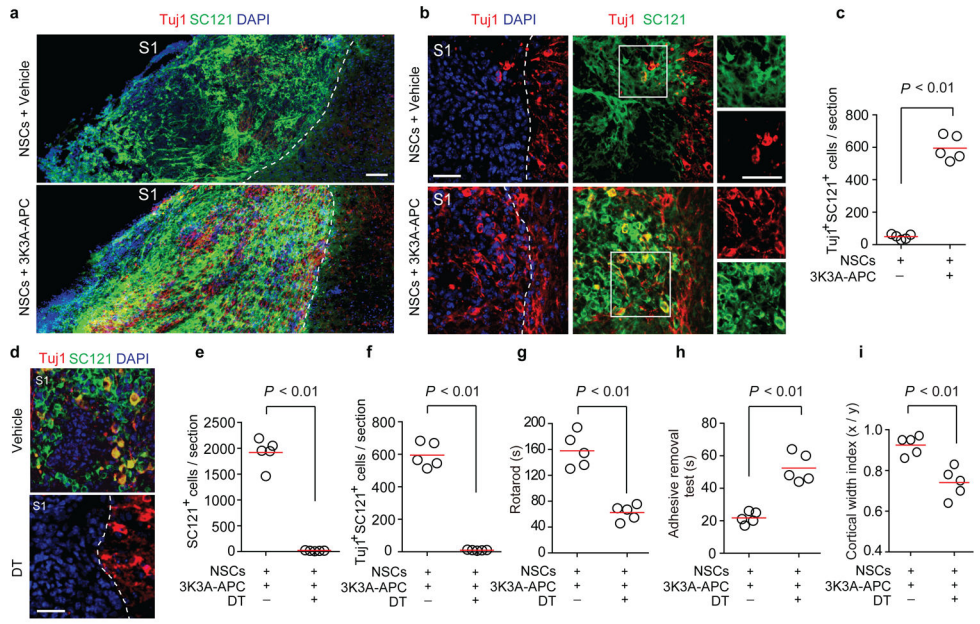

Figure 2. 3K3A-APC stimulates production of neuronal-like cells from transplanted NSCs after dMCAo

(**a**) Tiled fluorescent images of ischemia-affected region 35 d after dMCAo showing Tuj1 (red; neuronal marker) and SC121 (green, human antigen) co-immunostaining in mice treated with NSCs and vehicle or NSCs and 3K3A-APC. DAPI (blue), nuclear staining. Scale bar = 100 μm. S1, primary somatosensory cortex. (**b**) $Tuj1^+$ $SC121^+$ double positive cells from the affected S1 region 35 d after dMCAo and NSCs and vehicle (*top row*) or NSCs and 3K3A-APC (*bottom row*). Insets, individual channels from the boxed regions. Scale bar = 50 μm. (**c**) Scatter plot of $Tuj1^+$ $SC121^+$ double positive cells 35 d after dMCAo. n = 5 mice per group. (**d–f**) Images (**d**) and scatter plots (**e–f**) of engrafted $SC121^+$ cells and $Tuj1^+$ $SC121^+$ double positive cells in mice treated with NSCs and 3K3A-APC 7 d after intraperitoneal vehicle or diphtheria toxin (DT, 50 μg/kg) administered 35 d after dMCAo. Scale bar = 50 μm; n = 5 mice per group. (**g–i**) The rotarod test (**g**), adhesive removal test (**h**), and cortical width index (**i**) in mice treated with NSCs and 3K3A-APC followed by vehicle or DT 35 d after stroke. Behavior and cortical width measurements were performed 7 d after vehicle or DT. n = 5 mice per group. In **c** and **e–i,** significance by Student's-t test. In **a, b** and **d**, dotted lines, borders between ischemia-affected S1 region (*left*) and unaffected area (*right*).

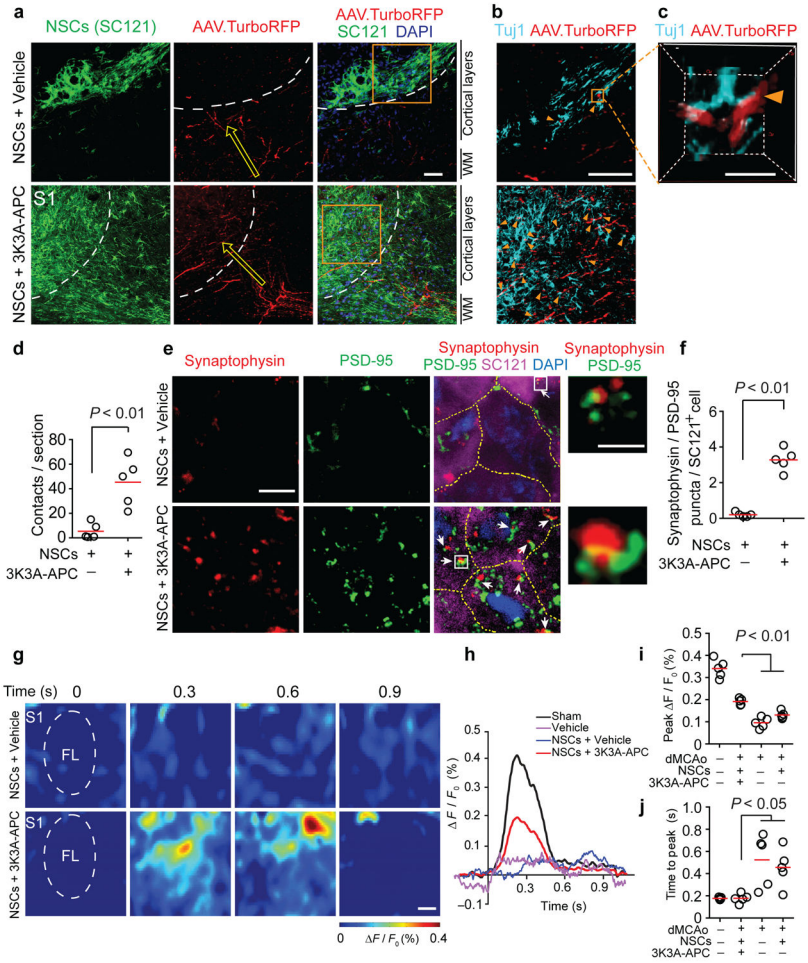

Figure 3. NSCs and 3K3A-APC combination therapy enables anatomical and functional improvements of dMCAo disrupted neural circuitry

(**a**) Viral-labeled axons projecting from the primary motor cortex (M1) to the somatosensory cortex (S1) 35 d after dMCAo. WM, white matter. Arrows, direction of axonal projections. Dotted lines, ischemia-affected border in the S1 region. Scale bar = 50 μm. (**b**) Tuj1$^+$ NSCs and viral-labeled axonal projections (AAV.TurboRFP) in the S1 boxed regions magnified from **a**. Arrowheads, TurboRFP$^+$ axons and Tuj1$^+$ NSCs points of contact. Scale bar = 50 μm. (**c**) 3D reconstruction of a point of contact in the boxed region (7 μm x 7 μm x 7 μm) magnified from **b**. Scale bar = 50 μm. (**d**) Scatter plot of TurboRFP$^+$ axons and Tuj1$^+$ NSCs contacts from **b–c**. *n* = 5 mice/group; significance by Student's-t test. (**e**) Synaptophysin (red; presynaptic marker) and PSD-95 (green; postsynaptic marker) co-localized puncta on SC121$^+$ NSCs in the S1 region (magenta). Arrows, co-localized puncta. Insets, high magnification of boxed regions showing co-localized puncta. DAPI (blue), nuclear staining; Scale bar = 5 main images, 1 μm insets. Dashed lines, borders between NSCs. (**f**) Scatter plot of synaptophysin and PSD-95 co-localized puncta on SC121$^+$ cells in the S1 region 35 d after dMCAo. *n* = 5 mice/group; significance by Student's-t test. (**g**) Voltage-sensitive dye (VSD) imaging of cortical responses to forelimb stimulation in NSCs and vehicle-treated (*top*) or NSCs and 3K3A-APC-treated (*bottom*) mice 35 d after dMCAo. Scale bar = 0.5

mm. FL, the forelimb somatosensory cortex. (**h–j**) VSD signal responses in the FL cortex (**h**), scatter plot of peak VSD amplitude (**i**) and time to peak response (**j**). $n = 5$ mice per group, significance by one-way ANOVA and Bonferroni's post hoc test.

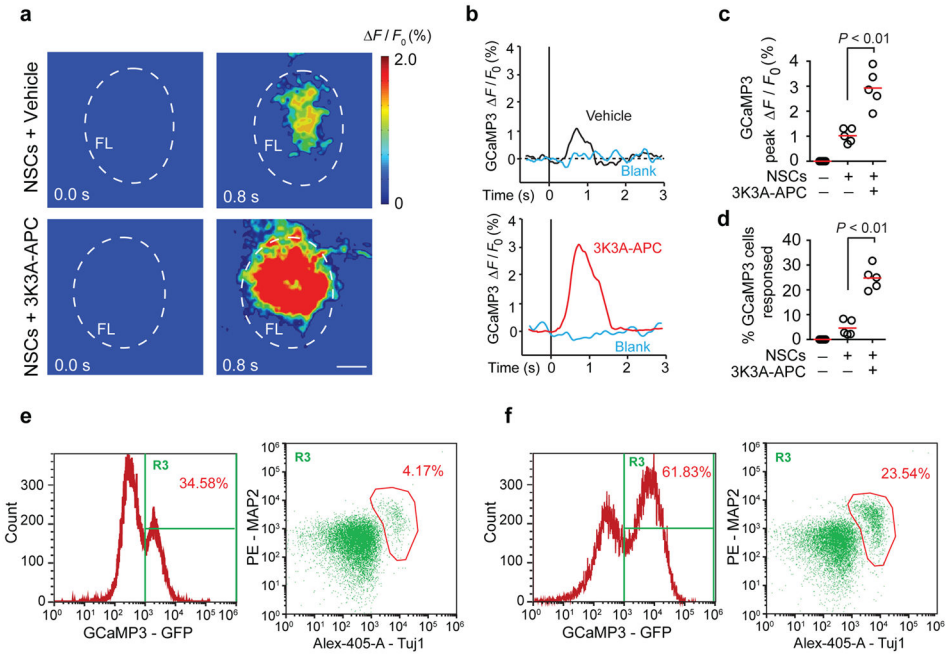

Figure 4. NSCs and 3K3A-APC combination therapy improves functional integration of the transplanted human NSCs

(**a**) Representative pseudo-colored frames from 5 mice per group showing the change in GCaMP3 fluorescence (Δ*F*/*F*) recorded through a cranial window over the primary somatosensory S1 cortex in response to forelimb stimulation 35 d after dMCAo. NSCs stably transduced with lentivirus carrying GCaMP3 were transplanted 7 d after dMCAo. Forelimb stimulation started at t = 0. Scale bar = 0.5 mm. The outlined region indicates the forelimb somatosensory cortex (FL). (**b**) Representative traces of GCaMP3 signal from GCaMP3-NSCs grafted in the primary sensory S1 cortex in response to forelimb stimulation. Blank traces indicate baseline with no stimulation. (**c**) Scatter plot of average peak change in fluorescence from experiments as in **b**. $n = 5$ mice per group; $P < 0.01$ by Student's t-test. (**d**) The percentage of GCaMP3-NSCs responding to forelimb stimulation as determined by *in vivo* two-photon imaging of individual GCaMP3-NSCs cell responses in the cortical layers II–III. $n = 5$ mice/group. $P < 0.01$ by Student's t-test. (**e–f**) Multicolor flow cytometry analysis of cell populations in the grafted cortical region of mice receiving NSCs and vehicle (**e**) or NSCs and 3K3A-APC (**f**) 35 d after dMCAo. Representative plots from 5 mice per group showing the percentage of GCaMP3-expressing NSCs (left) and the percentage of differentiated neuronal cells from GCaMP3-NSCs expressing neuronal markers MAP2 and Tuj1 (right).